Polymer Engineering & Science

TEMPERATURE, CONVERSION AND PHASE SEPARATION PROFILES DURING MOLD CURE OF A MODIFIED VINYLESTER RESIN

Journal:	*Polymer Engineering & Science*
Manuscript ID:	PES-06-0590.R1
Wiley - Manuscript type:	Research Article
Date Submitted by the Author:	02-Mar-2007
Complete List of Authors:	Schroeder, Walter; University of Mar del Plata, INTEMA auad, María; Auburn University, Polymer and Fiber Engineering Soulé, Ezequiel; University of Mar del Plata, INTEMA
Keywords:	phase separation, morphology, simulations

TEMPERATURE, CONVERSION AND PHASE SEPARATION PROFILES DURING MOLD CURE OF A MODIFIED VINYLESTER RESIN

Walter F. Schroeder[†], María L. Auad[‡] and Ezequiel R. Soulé[†*]

[†] Institute of Materials Science and Technology (INTEMA),

University of Mar del Plata – National Research Council (CONICET)

Av. Juan B. Justo 4302, (7600) Mar del Plata, Argentina

Tel: +54 (223) 481 66 00, FAX: +54 (223) 481 00 46

[‡] Polymer and Fiber Engineering Department, Auburn University

103 Textile Building, AL 36849, USA

Tel: 334.844.2308, FAX: 334.844.4487

* Corresponding author: ersoule@fi.mdp.edu.ar (E. Soulé)

ABSTRACT

In this work, morphological differences over the thickness of modified vinyl-ester (VE) samples are studied. A thermodynamic analysis based in the Flory-Rehner theory is proposed, in order to evaluate the spinodal decomposition temperature evolution during the reaction. This model takes into account changes in (styrene(St)-co-VE)copolymer composition and binary interaction parameters with conversion. Then, from the energy and mass balance equations, temperature and conversion profiles over the thickness as a function of reaction time are calculated. Combining these profiles with the proposed thermodynamic model, spinodal decomposition conversion graphs are constructed. In order to verify model predictions, a synthesized VE resin was modified with 7.5 wt% of poly(butadiene-co-acrylonitrile) vinyl terminated (VTBN) elastomer, and then cured in molds of 3, 7, 12 and 20 mm thickness at 80 ºC. Fracture surfaces were observed by scanning electron microscopy showing morphological differences over thickness, which can be explained from the results obtained from the simulation.

1. INTRODUCTION

Vinyl-ester (VE) is one of the most important thermosetting resins for composite formulations in industrial applications and in biomedical uses [1]. The materials formulated with these resins show valuable properties, such as excellent chemical resistance, thermal stability, and mechanical strength. Nevertheless, as it occurs with many thermoset polymers, a major drawback of VE matrices is its low fracture toughness [2, 3]. An usual method of toughening this materials is the modification with liquid rubbers, which induce a phase separation process during cure ("polymerization induced phase separation", PIPS) [4]. This method consists of preparing an initial homogeneous mixture of comonomers (VE and styrene (St)) and the additive. During the copolymerization (St-VE) a phase separation occurs because of the reduction of entropic contribution to the mixing Gibbs free energy due to the increase in the molecular weight of copolymer, the change in relative concentrations of the mixture components, and the increase in the degree of crosslinking. As the formed copolymer, St-VE, presents partial miscibility in the mixture, it begins to separate forming nodules called "microgels" in whose interior the crosslinking increases quickly [5-7]. At the same time that the VE and the St react, the monomeric phase gets rich in the liquid elastomer, and at the end of the curing reaction, the material is constituted by copolymer regions consisting of the aggregated nodules already formed, and elastomer rich regions. Depending on the amount of additive utilized, the final morphology corresponds to a matrix with irregular rubber inclusions or presents a co-continuous structure.

The resulting heterogeneous structure produces amplification of developed deformation mechanisms in material. Thus, the final morphology determined by the size, shape, and relative proportions of the domains of the phases present, influences significantly the

fracture toughness of the obtained material. Furthermore, other material properties, such as physical and thermal ones, are also affected by the final morphology.

Models which allow a very good description of PIPS process in modified systems polymerizing by a stepwise mechanism has been reported [4, 8-11]. For this polymerization type, statistical models which successfully describe the evolution of molar mass distribution as a function of reaction conversion have been developed. If presence of the modifier additive does not affect significantly the polymerization reaction, it is possible to combine the polymerization statistic model with a thermodynamic model, such as Flory-Huggins [12], in order to successfully describe the PIPS process.

Nevertheless, for systems polymerizing by a chainwise mechanism the development of a polymerization statistic model is highly complex. This fact is due to the formation of highly crosslinked nodules (microgels) containing numerous intramolecular rings which do not contribute to elastic properties of the network. Thus, in the few developed models, it has been necessary to introduce strong hypothesis on these aspects, so predictions are of qualitative nature [13].

In this work, we are presenting a thermodynamic model and a heat transfer analysis, which allows calculating temperature, conversion, and phase separation profile evolution during mold curing, and to infer morphological changes over sample thickness. Finally, the obtained results are compared with the final material morphologies observed by electron microscopy.

2. THEORETICAL BACKGROUND

2.1 Phase separation model

Thermodynamics of reactive network-forming systems can be analyzed with the model developed by Flory and Rehner for swollen gels [14], later modified by Dušek [15, 16]:

$$\Delta G = \Delta G_m + \Delta G_e \tag{1}$$

The entropic and enthalpic contribution to the mixing free energy, ΔG_m, is represented by the Flory-Huggins [17] lattice model, with a temperature dependent and composition independent interaction parameter χ ($\chi = a + b/T$, where a and b are constants). For a mixture of i components, this contribution is:

$$\frac{\Delta G_m}{MRT} = \sum_i \frac{\phi_i}{x_i} \ln \phi_i + \sum_{i,j} \chi_{ij} \phi_i \phi_j \tag{2}$$

where M is the number of moles of cells, R is the gas constant, T the absolute temperature, ϕ_i the volumetric fraction of i-species, and x_i the number of cells occupied by i-species. The cell volume was taken as 116.85 cm^3/mol, which corresponds to the molar volume of St monomer.

The elastic contribution, ΔG_e, which is present in the post-gel stage, can be represented by the following equation [13]:

$$\frac{\Delta G_e}{RTM} = \nu_e \varepsilon \phi_g \left[\frac{3}{2} \left(\phi_g^{-\frac{2}{3}} - 1 \right) + \frac{2}{f} \ln \phi_g \right] \tag{3}$$

where ϕ_g is the gel volumetric fraction, and $\nu_e \varepsilon \phi_g$ is the number of moles of elastic active chains per mol of cells. ν_e represents the number of chains between crosslinking points per mol of cells occupied by the gel; and ε indicates the fraction of this chains that have elastic behavior. This last parameter is introduced because rings or cycles are formed during the

polymerization reaction, both in pregel and postgel stages, and the chains forming these cycles do not participate of the elastic properties of the network.

Dušek [18] has reviewed publications about divinyl monomer homopolymerization and divinyl – monovinyl monomers copolymerization forming networks, and has concluded that ε can take values over large intervals, typically between 0.3 and 0.9; and it depends on divinyl monomer and rigidity of the polymer chain that forms the network. In this work, an arbitrary value within that range, $\varepsilon = 0.50$, was taken independently of VE concentration, as in ref [19].

To determine the number of crosslinking points, the same consideration made by Dušek [15] and Boots [13] was adopted. That is to suppose that all divinyl monomers with both insaturations reacted act like crosslinking points in the gel. Each insaturation of these divinyl monomers has a crosslinking functionality of $f = 3$. Then, ν_e is expressed by the following equation:

$$\nu_e = \frac{3}{2}\alpha_1^{\,2} f_{1,0} \tag{4}$$

where α_1^2 represents the probability that a reactive VE extreme belongs to a double reactioned VE molecule. $f_{1,0}$ is the initial molar fraction of VE insaturations, and the 3/2 factor represents the number of chains leaving a crosslinking point.

In all the simulations performed, phase separation took place after the gelation point. The Gibbs free energy of the homogeneous system is then:

$$[G]_{P,T,\alpha} = \frac{\Delta G}{RT} = \left(\begin{array}{l} \dfrac{\phi_0}{x_0}\ln\phi_0 + \dfrac{\phi_1}{x_1}\ln\phi_1 + \dfrac{\phi_3}{x_3}\ln\phi_3 + \chi_{01}\phi_0\phi_1 + \chi_{02}\phi_0\phi_2 + \\ + \chi_{03}\phi_0\phi_3 + \chi_{12}\phi_1\phi_2 + \chi_{13}\phi_1\phi_3 + \chi_{23}\phi_2\phi_3 + \\ + \nu_e\varepsilon\phi_g\left[\dfrac{3}{2}\left(\phi_g^{-\frac{2}{3}} - 1\right) + \dfrac{2}{3}\ln\phi_g\right] \end{array} \right) \tag{5}$$

where the subscripts represent: St(0), VE(1), copolymer(2), and modifier(3). In order to simplify, the entire polymer will be considered to form part of the gel phase, so $\phi_g = \phi_2$.

At any level of monomer conversion, in Liquid – Liquid or Liquid - Gel phase diagram, three zones can be defined: stable, metastable and unstable (spinodal). These zones are differenced by stability criteria for a homogeneous phase. In this work the effects of temperature, composition and conversion on phase transformation in the reactive St – VE – Copolymer – Modifier quaternary system were analyzed calculating the evolution of the spinodal decomposition temperature during the reaction. It was assumed that phase separation occurs when the spinodal condition is achieved. This is a reasonable hypothesis if phase separation occurs in the post-gel stage, because diffusional limitations in the crosslinked system make the phase separation process in the metastable zone to be very difficult, although it is still possible.

Spinodal condition is given by [12]:

$$Y = \left| \frac{\partial^2 \Delta G}{\partial \phi_i \partial \phi_j} \right|_{P,T,\alpha} = 0 \qquad (6)$$

where Y represents the determinant of Gibbs free energy second derivatives with respect to the independent compositions of the system. A homogeneous phase is unstable if $Y < 0$. In the region where $Y > 0$, a homogeneous phase may exist in stable or metastable conditions.

2.2 Heat Transfer model

The differential energy balance in rectangular coordinates, in a medium that is infinite in two directions and finite in the other, with constant physical properties and considering heat generation by chemical reaction is:

$$\frac{dT}{dt} = \frac{k}{\rho C_p}\frac{d^2T}{dz^2} + \frac{\Delta H}{C_p} r_p \tag{7}$$

where the parameters k, ρ, C_p, ΔH are the thermal conductivity, density, specific heat and reaction heat, respectively. The variables T, z and t are temperature, spatial dimension and time, respectively. r_p is the polymerization rate.

If there is no diffusion of chemical species, mass balance reduces to the expression for reaction rate:

$$\frac{d\alpha}{dt} = r_p \tag{8}$$

Equations (7) and (8), together with a kinetic model, define the time evolution and the spatial temperature and conversion profiles for the reactive system.

2.3 Kinetic model

Auad et. al [20] has studied the kinetics for this system, employing the Kamal phenomenological model [21, 22] with no significant initial polymerization rate:

$$\frac{d\alpha}{dt} = r_p = k\alpha^m (1-\alpha)^n \tag{9}$$

The copolymerization reaction St-VE can be described by Equation (9), as it has been shown by other authors [23-25].

The rate constant k is written taking into account the intrinsic chemical reaction rate (k_c) and the diffusional rate (k_d), using the Rabinowitch model [26].

$$\frac{1}{k} = \frac{1}{k_c} + \frac{1}{k_d} \tag{10}$$

k_c is written following the Arrhenius equation:

$$k_c = A\exp\left(\frac{-E}{RT}\right) \tag{11}$$

and k_d is written according the Vogel-Fulcher empirical equation [27]:

$$\ln(k_d) = \ln(k_{d0}) - \frac{E_d}{R}\frac{T_c}{T_g\left(T_c - T_g + 50\right)} \tag{12}$$

The change in glass transition temperature, T_g, can be calculated with the equation of Di Benedetto [28, 29], wich allows evaluating the T_g evolution with reaction conversion.

$$\frac{T_g - T_{g0}}{T_{g\infty} - T_{g0}} = \frac{\lambda\alpha}{1-(1-\lambda)\alpha} \tag{13}$$

In this equation, T_{g0} is the glass transition temperature at $\alpha = 0$ and $T_{g\infty}$ is the glass transition temperature at $\alpha = 1$. $\lambda = {\Delta C_{p\infty}}/{\Delta C_{p0}}$ is the ratio between specific heat change of the fully reacted and the initial system. When $\Delta C_p.T_g = constant$, then $\lambda = {T_{g0}}/{T_{g\infty}}$, [29]. This last relation was used in this work.

3. SIMULATION METHODS

In order to solve heat transfer equations, MOLCH subroutine of IMSL library, in Fortran Power Station 4.0, was used. In this subroutine, the method of the lines is used. The position was discretized considering 500 points. Initial time integration step selected was $4*10^{-7}$ seconds. It was considered that reaction kinetics is not affected by the presence of the modifier.

Initial and boundary conditions used were:

$t < 0$	$T = 353$ K	$\forall z$
$z = 0$, $z = L$	$T = 353$ K	$\forall t$
$t = 0$	$\alpha = 0$	$\forall z$

Equation (9) requires the initial conversion to be non-zero. The same value used in the determination of kinetic parameters [20] (0.0001) was used in the calculations.

In order to solve the thermodynamic model, it is necessary to relate concentrations of St, VE and copolymer (as well as its composition and molar mass), with global conversion which is calculated from equation (9).

It was considered that an initial number of moles, N_0, reacted in N_0 steps (one mol per step). Ignoring the effects of modifier, the St molar fraction in the copolymer, for a step i, can be calculated from a general balance:

$$F_{0,i} = \frac{r_0 f'_{0,i-1} + f'_{0,i-1} f'_{1,i-1}}{r_0 f'^2_{0,i-1} + 2 f'_{0,i} f'_{1,i-1} + r_1 f'^2_{1,i-1}} \tag{14}$$

The subscripts 0 and 1 have been used for St and VE respectively. The reactivity ratios, r_0 and r_1, were taken as constants. The f' are molar fractions in the comonomer bulk.

$$f'_{0,i} = \frac{[N_0 - (i-1)] f'_{0,i-1} - F_{0,i}}{N_0 - i} \qquad f'_{1,i} = 1 - f'_{0,i} \tag{15}$$

With equations (14) and (15) f and F can be calculated for each reaction step. Conversions of both reactants and global conversion can then be calculated:

$$\alpha_{0,i} = \alpha_{0,i-1} + \frac{F_{0,i}}{N_0 f'_{0,0}} \qquad \alpha_{1,i} = \alpha_{1,i-1} + \frac{F_{1,i}}{N_0 f'_{1,0}} \tag{16}$$

$$\alpha_i = \frac{\alpha_{0,i} f'_{0,0} + \alpha_{1,i} f'_{1,0}}{f'_{0,0} + f'_{1,0}}$$

Finally, it is necessary to calculate the interaction parameters between the copolymer and the other species, which can be calculated from the segmental interaction parameters [30]. In a mixture of a homopolymer A and a random copolymer B_xC_{1-x}, interaction parameter between homopolymer and copolymer can be written as:

$$\chi_{ACopol} = \phi^c{}_B \chi_{AB} + \left(1 - \phi^c{}_B\right)\chi_{AC} - \phi^c{}_B\left(1 - \phi^c{}_B\right)\chi_{BC} \tag{17}$$

In this case the following segmental interaction parameters are needed:

$$\begin{aligned} &\chi_{\text{St-HVE}} = \chi_{\text{HSt-VE}} = \chi_{0\text{-}1} \\ &\chi_{\text{HVE-VTBN}} = \chi_{1\text{-}3} \\ &\chi_{\text{HSt-VTBN}} = \chi_{0\text{-}3} \end{aligned} \tag{18}$$

HVE and HSt represent the segments of VE and St in the copolymer, and are assumed to be equivalent to the monomers. The subscript 3 represents the modifier. The third therm of equation (18) requires the knowledge of the interaction parameter HSt – HVE, which is taken as [19]:

$$\chi_{HSt-HVE} = \chi_{St-VE,critic} K = \frac{2}{x_{2,0}} K \tag{19}$$

$x_{2,0}$ is the average size of HVE or HSt, considered equal to the size of the copolymer at zero conversion. This value was taken from Okay et. al.[31], and is 1950. K is an empirical parameter, considered equal to 10 [19].

So, the resulting equations are:

$$\begin{aligned} \chi_{02,i} &= \phi c_{1,i}\chi_{10} - \phi c_{0,i}\phi c_{1,i}\chi_{10} \\ \chi_{12,i} &= \phi c_{0,i}\chi_{10} - \phi c_{0,i}\phi c_{1,i}\chi_{10} \\ \chi_{23,i} &= \phi c_{0,i}\chi_{30} + \phi c_{1,i}\chi_{13} - \phi c_{0,i}\phi c_{1,i}\chi_{10} \end{aligned} \tag{20}$$

Considering that the total volume does not change upon reaction, the volumetric fraction of each monomer in the copolymer are:

$$\phi^{c}{}_{0,i} = \frac{\alpha_{0,i}\dfrac{f_{0,0}M_0}{\rho_0}}{\alpha_{0,i}\dfrac{f_{0,0}M_0}{\rho_0} + \left(\alpha_{1,i}^2 + 2\alpha_{0,i}\alpha_{1,i}\right)\dfrac{f_{1,0}M_1}{\rho_1}} \qquad \phi^{c}{}_{0,i} = 1 - \phi^{c}{}_{0,i} \qquad (21)$$

With previous equations, spinodal temperature could be calculated for the global conversion corresponding to each reaction step.

4. EXPERIMENTAL

4.1. Materials and sample preparation

A vinyl ester (VE) monomer was synthesized by reacting an epoxy resin, diglycidyl ether of bisphenol A (DGEBA, DER 332, Dow Chemical Co.; epoxy equivalent weight 175 g/eq) with methacrylic acid (Norent Plast S.A., Buenos Aires, Argentina, laboratory-grade reagent) and triphenylphosphine (Fluka A.G., Switzerland; analytical reagent) as catalyst [32]. The final conversion reached (monitored by titration of residual acid groups and by FTIR (Mattson Genesis II)) was higher than 97%, and the final product was stabilized with 500 ppm of hydroquinone. The obtained VE monomer was characterized by FTIR and ^{1}H-NMR (Bruker AM-500) spectroscopies [32, 33], and its molecular weight was measured by SEC chromatography (SEC) (waters Model 440, with columns PLGel of 100, 500, 10^3, 10^4, and 10^6 Å) in distilled tetrahydrofuran (Laboratorios Cicarelli, Argentina; analytical reagent) with a flow rate of 1 ml/min, using polystyrene calibration. Finally, its density was measured using a precision balance (Becker and Sons).

The liquid rubber additive was obtained from BF Goodrich Co., vinyl terminated poly(butadiene-co-acrylonitrile) (VTBN, 1300 x 33). The characterization of the used components is summarized in Table 1.

The crosslinked samples were prepared maintaining a proportion of 55-45% by weight of VE to styrene (St) (Poliresinas San Luis S.A., Argentina; laboratory-grade reagent), as it is commonly used commercially, using benzoyl peroxide 2 wt% (Lucidol 75%, Akzo Chemicals S.A., Buenos Aires, Argentina) as initiator, and with 5 wt% of VTBN as modifier. All the reagents were used as received.

Samples of different thickness were obtained by casting the mixture into molds consisting of two glass plates coated with a silicone release agent, spaced by a rubber cord of required thickness, and held together with clamps. The samples were cure at 80 ºC for 2 hours. After the curing process, the samples were cooled slowly in the oven.

4.2. Electron microscopy

Micrographs of the fracture surfaces of the different materials were recorded using a scanning electron microscope operated at 15 kV (Cambridge 360 SEM). Fractured specimens were coated with gold to impart electrical conductivity.

5. RESULTS AND DISCUSSION

The predictive capabilities of the developed model were demonstrated by using it to calculate the temperature, conversion, and phase separation profile evolution during mold cure of a vinyl-ester resin modified with VTBN. Table 2 summarizes the physical parameters used in the calculations, and Table 3 includes the values of the binary

interaction parameters. In what follows, model predictions are compared with the final material morphologies observed by scanning electron microscopy.

The simulated curing results from a 3 mm thickness sample show flat temperature, conversion and phase separation profiles for all times analyzed. In this case the phase separation conversion was about 0.185 for any position on thickness.

Figures 1(a) and (b) show calculated temperature and conversion profiles, respectively, during cure in a 7mm in thickness mold. In this case heat dissipation rate is not high enough to keep the system in isothermal condition. The existence of a temperature profile implies different reaction rates at different positions in the samples thickness and then conversion profiles are produced. Figures 1(c) and (d) show phase separation time and conversion, respectively. As it can be observed, phase separation profiles are not very sharp because phase separation begins when temperature and conversion profiles are not still developed.

Conversion and temperature profiles for 12mm in thickness are shown in Figures 2(a) and (b). The temperature reached is higher than in the case of 7mm, and the profiles develop faster. Although these profiles are apparently similar in shape to the ones corresponding to the previous case, there are some important differences. Due to the high thickness of the sample, the resistance to heat dissipation is very important. The temperature in the central zone rises very fast, producing an inflection point in positions between the centre and the extremes. Between the inflection point and the centre, the second derivative of temperature respect to the position is negative, so heat is loosed by conduction. On the other hand, between the inflection point and the extremes, the second derivative is positive, so heat is gained by conduction. As a result, different positions follow very different trajectories in a temperature-conversion diagram, as it can be seen in

Figure 2(c). In the intermediate and extreme positions, after that the inflection point is generated, heat is gained by conduction (in addition to heat generated by reaction), increasing the temperature rise. Then, as the inflection point moves towards the extremes, the second derivative in these positions decrease and becomes negative. In this stage temperature rise is less pronounced.

An important fact that arises from Figure 2(c), is that different positions intercept spinodal curve at different conversion. As a consequence of this, profiles of phase separation conversion are generated. Figures 2(d) and (e) show profiles of phase separation time and conversion, respectively. It is interesting to notice that at intermediate positions the spinodal curve is not intercepted during the reaction, this only happens in the latest stage of the process, when the reaction has finished and the system is cooling.

Figures 3(a) and (b) show calculated temperature and conversion profiles, respectively, during cure in a mold of 20 mm in thickness. These profiles are very sharp, but unlike to the previous case, two temperature and conversion maxima are observed in positions between the centre and the extremes. The reason for this is that, due to large thickness, during the heating stage the temperature in the center of the mold rises much slower than in the extremes, so the reaction begins later in the central zone. As it can be observed in Figures 3(c) and (d), phase separation begins at the extremes, while in the central region spinodal curve is intercepted after that the reaction has finished.

The analyzed profiles allow us to explain the observed morphological changes over thickness for the final materials cured in different molds.

Figure 4 shows the SEM micrograph of the fracture surface for the modified material cured in a 3 mm in thickness mold. This morphology is similar to that observed by Auad et al [34] for a vinyl-ester system modified with VTBN, where a phase separated structure

with irregular rubber domain dispersed into a VE-St matrix was presented. The same morphology is observed at different position on sample thickness, as it is expected from the predicted flat profiles of temperature and conversion.

SEM micrographs of the fracture surface corresponding to a mold 7 mm in thickness at different positions are shown in Figures 5. As it can be observed, the morphology in the central region is clearly different from that corresponding to the extremes (wall). Similar morphological differences were observed in a vinyl-ester system modified with a thermoplastic additive at different cure temperatures [35]. Lower temperature morphologies show smaller copolymer nodules surrounded by the modifier, and higher temperature ones are characterized by larger copolymer nodules. This could be explained considering that higher temperature means lower viscosity during the phase separation process, and as a consequence larger nodules. As it can be seen in Fig. 5 smaller copolymer nodules can be observed in the wall regions (lower temperature morphology), while in the central region the nodules are larger (higher temperature morphology). This can be expected from the profiles shown in Figure 1(a), where it is observed that the central zone temperature is higher than that in the extremes.

Figure 6 shows SEM micrographs of fracture surface corresponding to a mold 12 mm in thickness, at different positions. As in the previous case, morphologies of high and low temperature are observed in centre and wall, respectively. It was shown in Figure 2(d) that, for intermediate zones, the spinodal condition is reached after the reaction is completed, when the sample is cooling. According to this, it could be expected that no phase separation takes place because of diffusion restrictions to phase separation (the material is highly crosslinked and the temperature is close to T_g). Nevertheless, the system may phase-separate if it enters the metastability region (that is, if it intercepts the binodal curve), and

this can happen without intercepting the spinodal. Although it was not observed experimentally, it is interesting to note that, theoretically, for certain conditions it could be the case that a material is phase separated in the centre and in the extremes, and homogenous between, when cured in thick molds.

In the case of a mold 20 mm in thickness, a more interesting behavior is observed. Different morphologies are developed in the centre, walls and intermediate positions, as is can be observed in Figure 7. A heterogeneous structure is observed in the extremes, like low temperature previous morphologies, consistently with the model predictions. The intermediate high temperature regions shows a morphology characterized by larger copolymer nodules conforming the main matrix phase. An interesting finding is that SEM micrograph of the central region shows a much less irregular surface, indicating that phase separation process is not very developed. In Figure 3(c) it was shown that spinodal curve is intercepted during cooling, after the reaction is finished. As in the previous case, the binodal curve must be intercepted, so phase separation takes place, but in lower degree.

It is important to emphasize that, despite the simplicity of the proposed model, it allows to explain some of the morphological changes experimentally observed on the cured samples within molds of different thickness. These morphological differences should be taken into account when planning isothermal cure of thick parts.

6. CONCLUSIONS

An analysis of polymerization induced phase separation in molds of different thickness, based on thermodynamic and heat transfer models, was performed for a VTBN modified vinyl ester resin cured at constant mold temperature. The temperature, conversion, and

phase separation profile evolution during cure were calculated in order to explain morphological changes observed over thickness.

Thin samples showed uniform morphologies in agreement with the flat profiles predicted by the model. As thickness is increased, a maximum in conversion and temperature is developed at the center generating different morphologies in central and wall regions; the first corresponding to higher temperature and the second to lower temperature. This was observed by SEM micrographs taken at different positions.

For large thickness (20 mm) two maxima of temperature exist in positions between the centre and the extremes. The model predicts that spinodal in the central region is not intercepted up to the cooling stage, whereas the intermediate regions and the walls get into the spinodal region at lower conversions. Under these conditions, three different morphologies are generated. A lower temperature morphology in the extremes, a higher temperature morphology in the intermediate regions, and a less heterogeneous morphology at the centre.

A remarkable model prediction for an intermediate thickness (12 mm) is the possibility of getting a material phase separated in the walls and the centre, and homogeneous between. This was not seen experimentally, but it is interesting to find that given appropriated conditions this could happen.

ACKNOWLEDGEMENTS

The financial support of Argentine institutions for promoting the science and technology CONICET, ANPCyT and the National University of Mar del Plata are greatly acknowledged.

REFERENCES

1. S.H. Zawke, *Thermosetting Resins,* S.H. Goodman ed., Noyes Publications, New Jersey (1986).

2. J.P. Pascault and R.J.J. Williams, *Polymer Blends, Volume I: Formulation and Characterization of Thermoset-Thermoplastic Blends,* D.R. Paul and C.B. Bucknall eds., John Wiley and Sons, New York (2000). Advances in Chemistry Series 233.

3. L. Suspense, Y.S. Yang, J.P. Pascault, *Toughened Plastics I: Science and Engineering,* C.K. Riew, A.J. Kinloch, eds., American Chemical Society, Washington DC (1993).

Flory P. J., and Rehner J.; *J. Chem. Phys.*, 11, 521 (1943).

4. R.J.J Williams, B.A. Rozenberg, J.P. Pascault, *Adv. Polym. Sci.,* **128**, 97 (1997).

5. R.P. Brill, G.R. Palmese, *J. Appl. Polym. Sci.,***76**, 1572 (2000).

6. A.R. Kannurpatti, K.J. Anderson, J.W. Anseth, C.N. Bowman, *J. Polym. Sci., Part B: Polym. Phys.*, **35**, 2297 (1997).

7. L. Rey, J. Galy, H. Sautereau, *Macromolecules*, **33**, 6780 (2000).

8. W.H. Ho, M.B. Ko, *Macromolecules,* **27**, 7815 (1994).

9. C.C. Riccardi, J. Borrajo, L. Meynie, F. Fenouillot, J.P. Pascault, *J. Polym. Sci., Part B: Polym. Phys.*, **42**, 1351 (2004).

10. C.C. Riccardi, J. Borrajo, L. Meynie, F. Fenouillot, J.P. Pascault, *J. Polym. Sci., Part B: Polym. Phys.*, **42**, 1361 (2004).

11. M.J. Galante, J. Borrajo, R.J.J Williams, E. Gyrard-Reydet, J.P. Pascault, *Macromolecules*, **34**, 2686 (2001).

12. K. Kamide, *Thermodynamic of Polymer Solutions: Phase Equilibria and Critical Phenomena*, A.D. Jenkins ed., Elsevier, Amsterdam, Holland, (1990). Polymer Science Library 9.

13. H.M. Boots, J.G. Kloosterboer, C. Serbutoviez, F.J. Tounslager, *Macromolecules*, **29**, 7683 (1996).

14. P.J. Flory, J. Rehner, *J. Chem. Phys.*, **11**, 521 (1943).

15. K. Dušek, *J. Polym. Sci.*, **16**, 1289 (1967).

16. K. Dušek, M. Dušková-Smrčková, *Prog. Polym. Sci.,* **25**, 1215 (2000).

17. P.J. Flory, *Principles of Polymer Chemistry*, Cornell University, Ithaca (1953).

18. K. Dušek, *Polymer Network: Structural and Mechanical Properties*, A.J. Chompff ed., Plenum Press, New York (1971).

19. M.L. Auad, Doctoral thesis: *Síntesis, caracterización y propiedades de materiales a partir de resinas vinil-éster*, National University of Mar del Plata, Argentina (1999).

20. M.L. Auad, M.I.Aranguren, G. Eliçabe, J. Borrajo, *J. Appl. Polym. Sci,***74**, 1044 (1999)

21. M.R. Kamal, S. Sourour, *Polym. Eng.. Sci.;* **13**, 59 (1973).

22. M.R. Kamal, *Polym. Eng.. Sci.;* **14**, 231 (1974).

23. J.H. Lee, J.W. Lee, *Polym. Eng. Sci.*, **34**, 741, (1994).

24. R. Chandra, R.K. Soni, *Polym. Intern.,* **31**, 236, (1993).

25. R. Chandra, R.K. Soni, *Polymer Intern.,,* 38, 147, (1995).

26. E.. Rabinowitch, *Trans. Faraday Soc.*, **33**, 1225, (1937).

27. G.A. Fulcher, *J. Am. Ceram. Soc.;* **8**, 339 (1925).

28. G. Wisanrakkit, J. Gillham, *J. Appl. Polym. Sci.,* **41**, 2885 (1990).

29. J.P.Pascault, R.J.J. Williams, *J. Polym. Sci. Part B: Polym. Phys.,* **28**, 85 (1990).

30. G.D. Merfeld, D.R. Paul, *Polymer Blends, Volume I: Formulation and Characterization of Thermoset-Thermoplastic Blends,* D.R. Paul and C.B. Bucknall eds., John Wiley and Sons, New York (2000). Advances in Chemistry Series 233.

31. O. Okay, M. Kurz, K. Lutz, W. Funke, *Macromolecules*, **28**, 2728 (1995).

32. M.L. Auad, M.I. Aranguren, J. Borrajo, *J. Appl. Polym. Sci.,* **66**, 1059 (1997).

33. S. Ziaee, G.R. Palmese, *J. Polym. Sci. Part B: Polym. Phys.,* **37**, 725 (1999).

34. M. L. Auad, P.M. Frontini, J. Borrajo, M.I. Aranguren, *Polymer*, **42**, 3723 (2001).

35. W.F. Schroeder, Doctoral thesis: *Modificación de Resinas Vinil-Ester con Polímeros Termoplásticos: Separación de Fases, Morfologías, y Propiedades Finales*, National University of Mar del Plata, Argentina (2006).

36. L. Li, X. Sun, L.J. Lee, *Polym. Eng. Sci.*, **39**, 646, (1999).

37. M.L Auad, M.I Aranguren, J. Borrajo, *Polymer*, **42**, 6503 (2001).

FIGURE CAPTIONS

Figure 1. Calculated profiles during cure in a mold 7 mm in thickness: (a) temperature; (b) conversion; (c) phase separation time; (d) phase separation conversion.

Figure 2. Results for cure in a mold 12 mm in thickness: (a) temperature profiles; (b) conversion profiles; (c) Temperature-conversion trajectories at different positions (the distance from the wall, in mm, is indicated on each curve). Dashed line represents the spinodal curve. (d) phase separation time profiles; (e) phase separation conversion profiles.

Figure 3. Results for cure in a mold 20 mm in thickness: (a) temperature profiles; (b) conversion profiles; (c) Temperature-conversion trajectories at different positions (the distance from the wall, in mm, is indicated on each curve). Dashed line represents the spinodal curve. (d) phase separation time profiles; (e) phase separation conversion profiles.

Figure 4. SEM micrograph of the fracture surface for the VTBN modified vinylester sample cured within a mold 3 mm in thickness.

Figure 5. SEM micrographs, at different thickness positions, of the fracture surface for the VTBN modified vinylester sample cured within a mold 7 mm in thickness.

Figure 6. SEM micrographs, at different thickness positions, of the fracture surface for the VTBN modified vinylester sample cured within a mold 12 mm in thickness.

Figure 7. SEM micrographs, at different thickness positions, of the fracture surface for the VTBN modified vinylester sample cured within a mold 20 mm in thickness.

Table 1. Physicochemical characteristics of the used components.

	St (0)	VE (1)	VTBN (3)
M_n (g/mol)	104	583	3600
M_w / M_n	—	1.06	1.81
Density$_{25\,°C}$ (g/cm^3)	0.89	1.16	1.06

Table 2. Physical parameters of the St-VE reactive system, modified with 7.5 wt% VTBN, used in the calculations.

C_p (J/g ºC)	k (J/m s ºC)	ΔH (J/g)	T_{g0} (K)	$T_{g\infty}$ (K)
1.5[a]	0.17[a]	364.0[a]	178[b]	398[b]

[a] Taken from ref. [36].

[b] Measured by differential scanning calorimetry (Shimadzu, DSC-50).

Table 3. Constants *a* and *b* of the interaction parameter equation [37]

	A	*b* (K)
St - VE	-0.078	77.27
St - VTBN	-0.149	45.90
VE - VTBN	-0.003	18.27

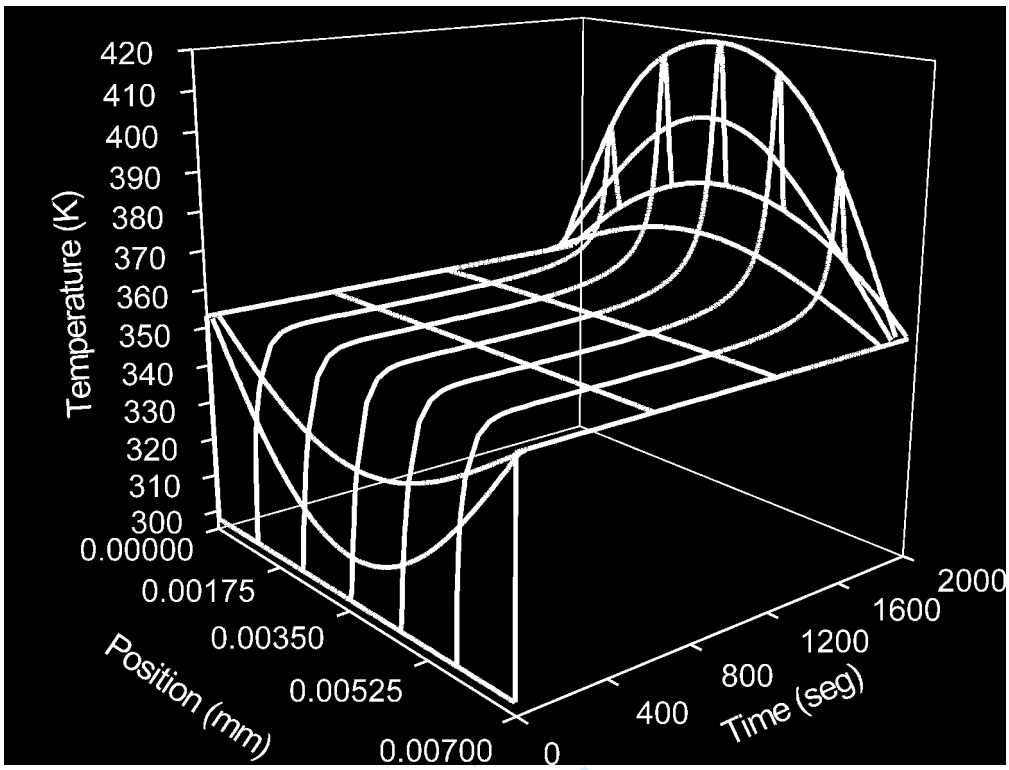
Temperature (K)
420
410
400
390
380
370
360
350
340
330
320
310
300
Position (mm)
0.00000
0.00175
0.00350
0.00525
0.00700
Time (seg)
0
400
800
1200
1600
2000

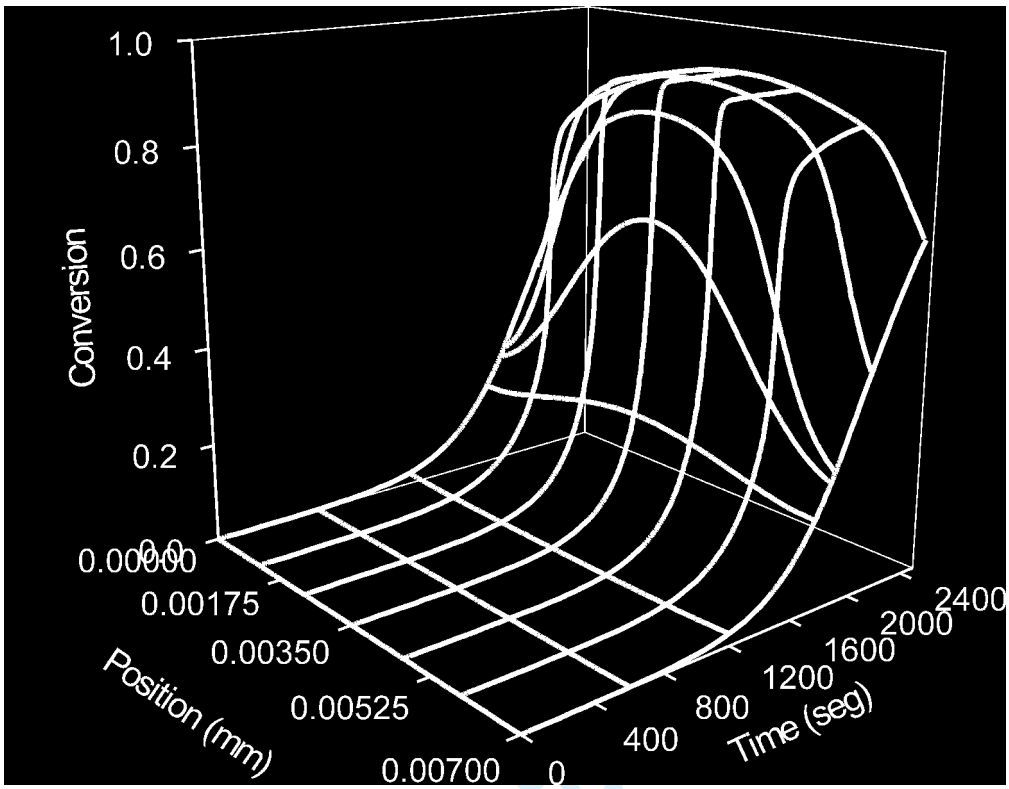
1.0
0.8
0.6
0.4
0.2
0.0
Conversion
0.00000
0.00175
0.00350
0.00525
0.00700
Position (mm)
0
400
800
1200
1600
2000
2400
Time (seg)

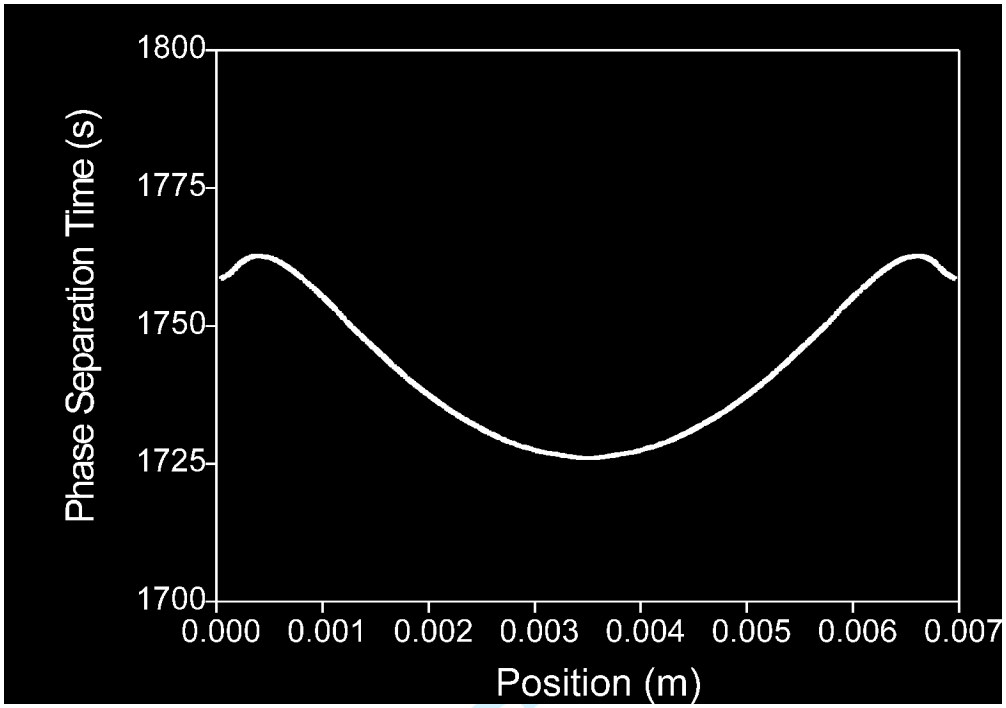
Phase Separation Time (s)
1800
1775
1750
1725
1700
0.000
0.001
0.002
0.003
0.004
0.005
0.006
0.007
Position (m)

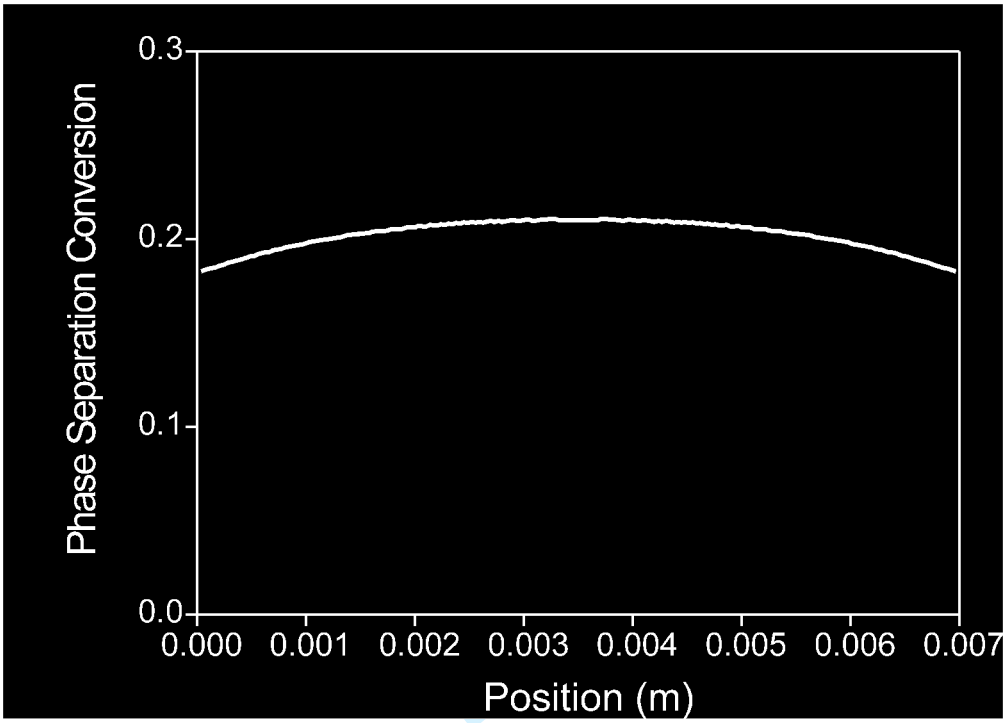
Phase Separation Conversion
0.3
0.2
0.1
0.0
0.000
0.001
0.002
0.003
0.004
0.005
0.006
0.007
Position (m)

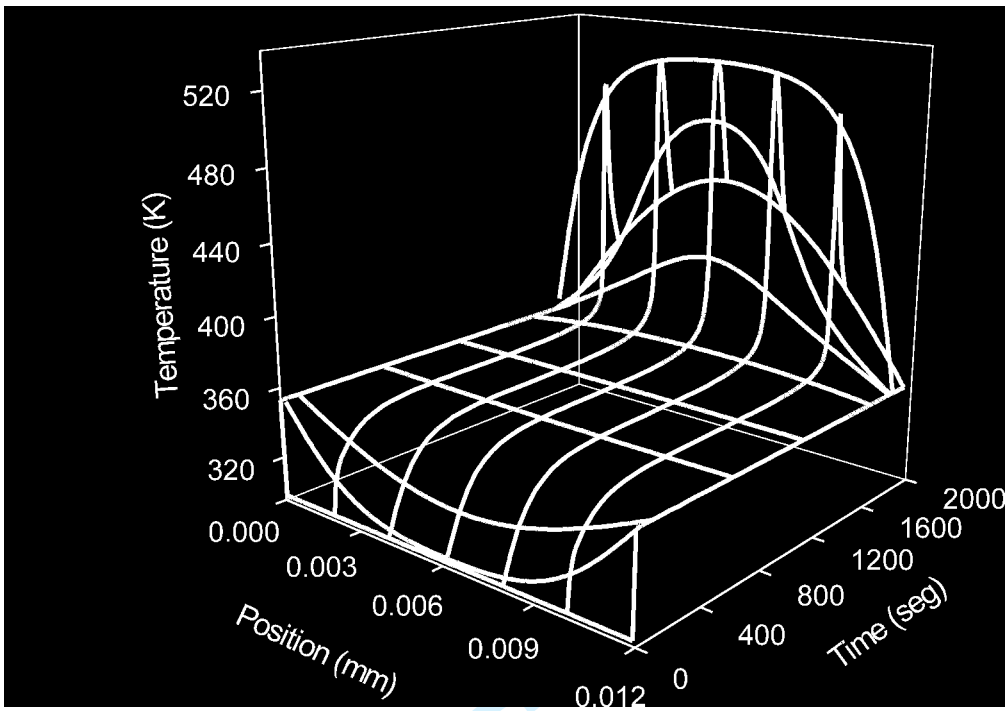
Temperature (K)
520
480
440
400
360
320
0.000
0.003
0.006
0.009
0.012
Position (mm)
0
400
800
1200
1600
2000
Time (seg)

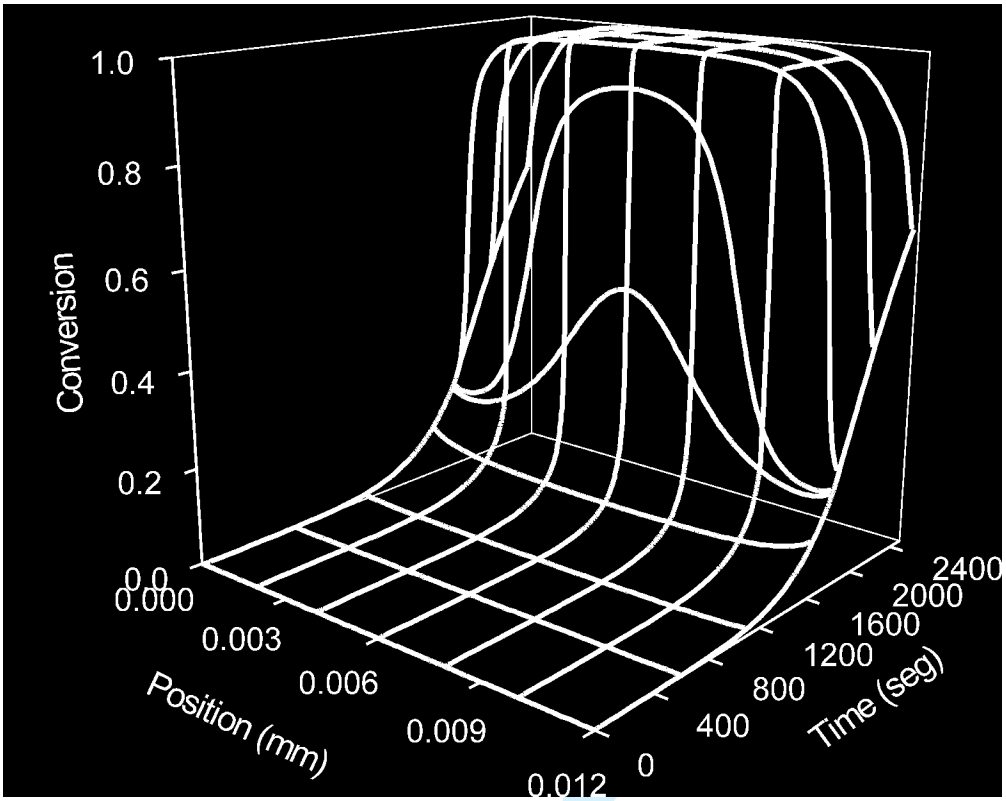
Conversion
1.0
0.8
0.6
0.4
0.2
0.0
0.000
0.003
0.006
0.009
0.012
Position (mm)
0
400
800
1200
1600
2000
2400
Time (seg)

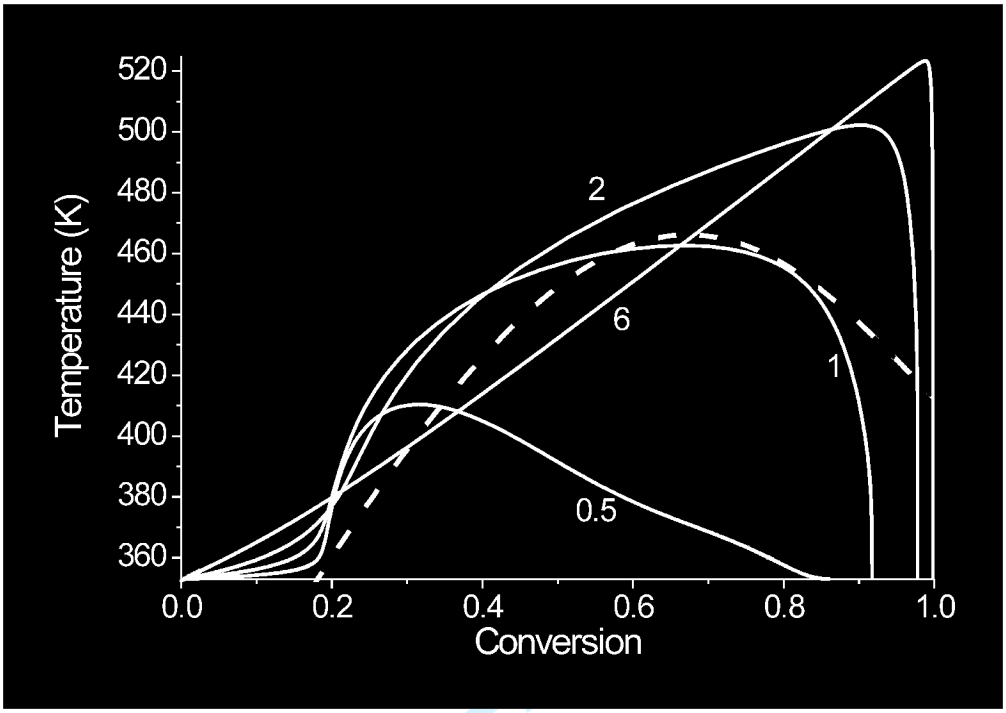
Temperature (K)
520
500
480
460
440
420
400
380
360
0.0
0.2
0.4
0.6
0.8
1.0
Conversion
2
6
1
0.5

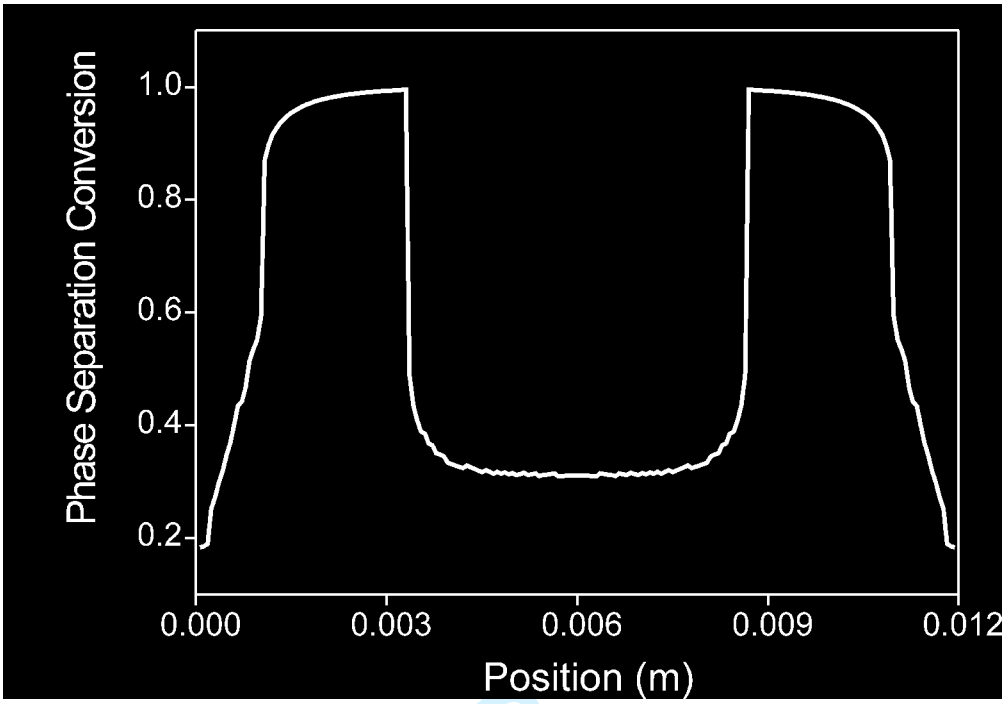
Phase Separation Conversion
1.0
0.8
0.6
0.4
0.2
0.000
0.003
0.006
0.009
0.012
Position (m)

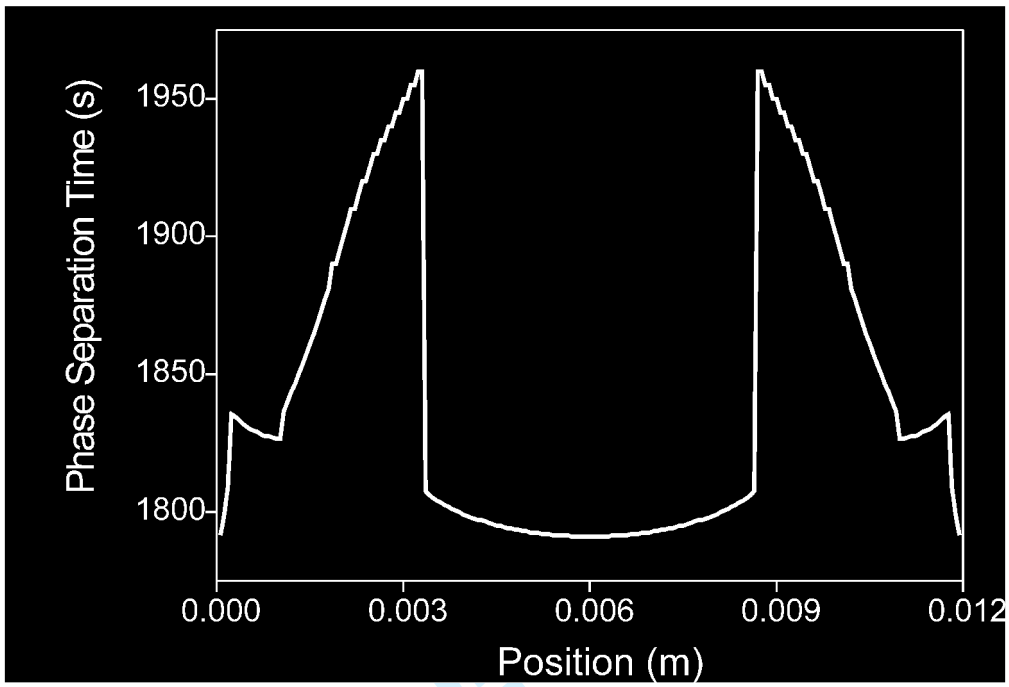

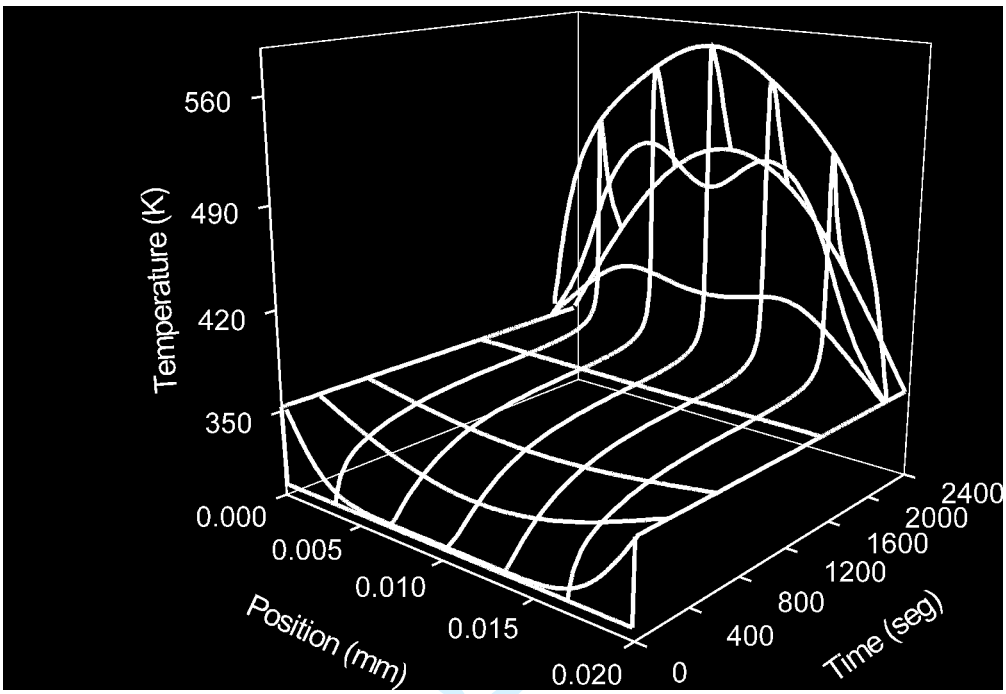
Temperature (K)
560
490
420
350
0.000
0.005
0.010
0.015
0.020
Position (mm)
0
400
800
1200
1600
2000
2400
Time (seg)

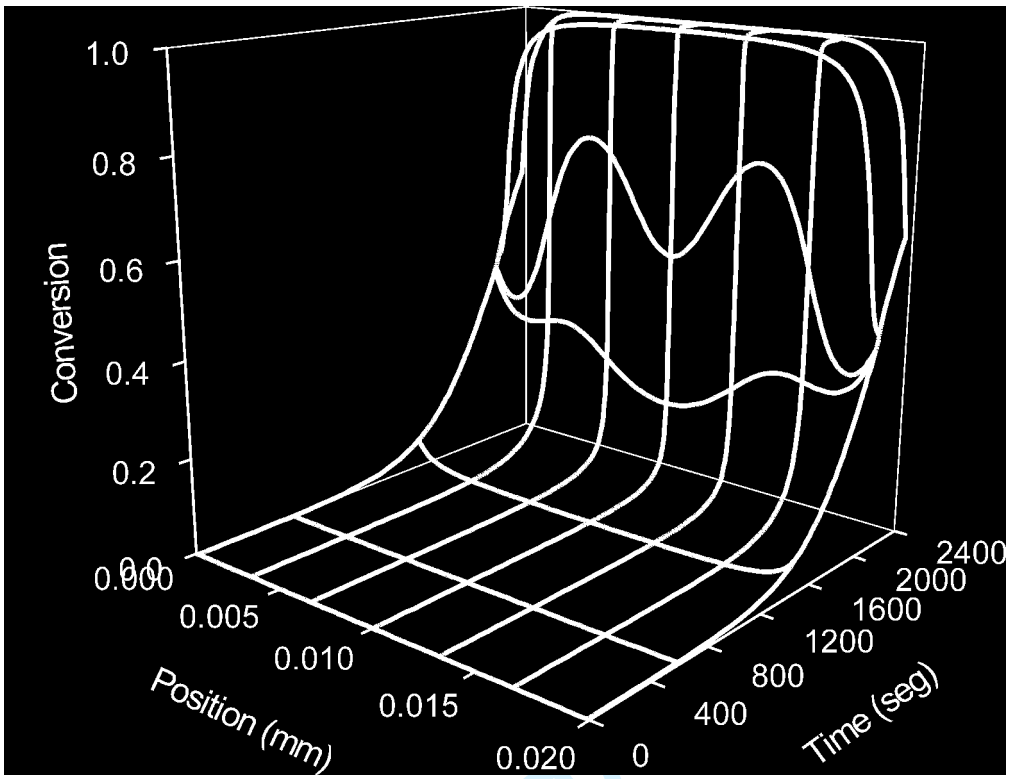
Conversion
1.0
0.8
0.6
0.4
0.2
0.0
0.000
0.005
0.010
0.015
0.020
Position (mm)
0
400
800
1200
1600
2000
2400
Time (seg)

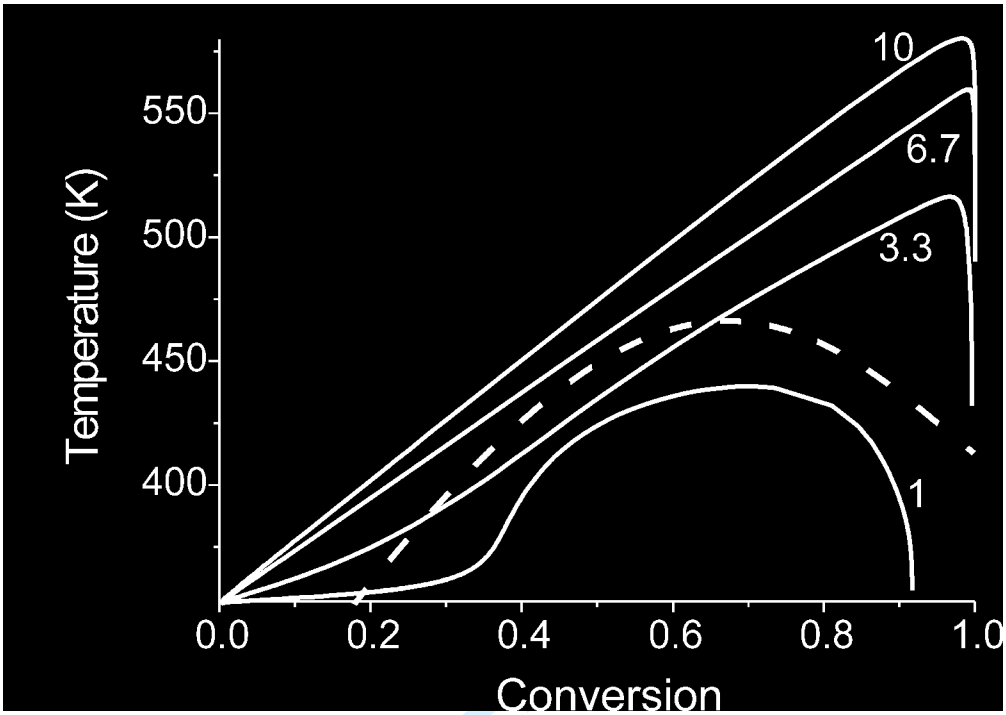
Temperature (K)
550
500
450
400
0.0
0.2
0.4
0.6
0.8
1.0
Conversion
10
6.7
3.3
1

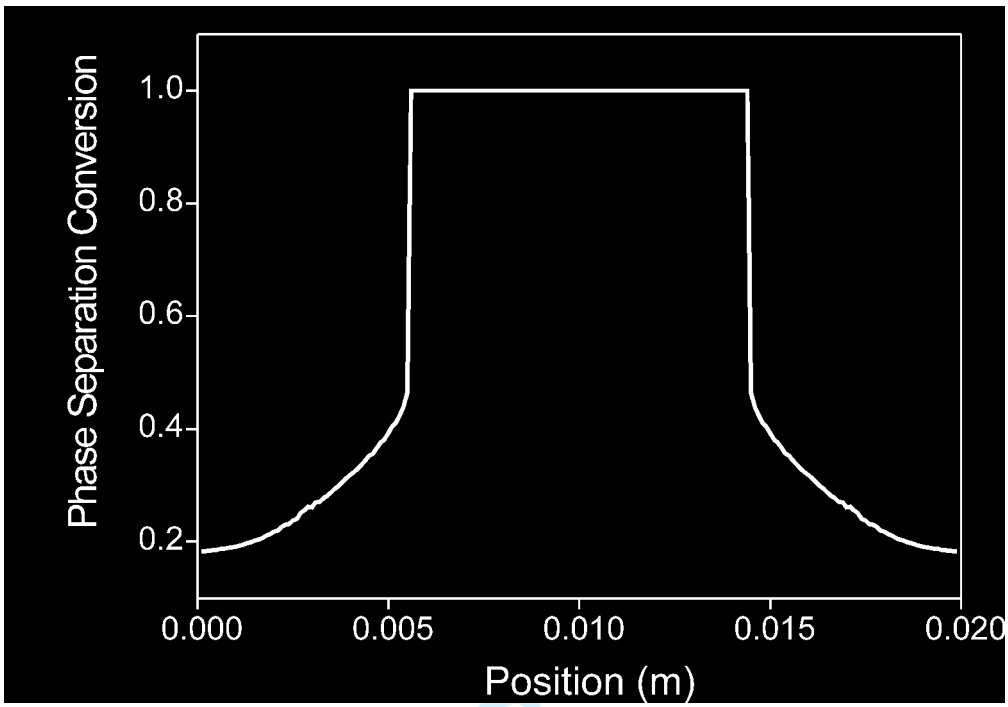
Phase Separation Conversion
1.0
0.8
0.6
0.4
0.2
0.000
0.005
0.010
0.015
0.020
Position (m)

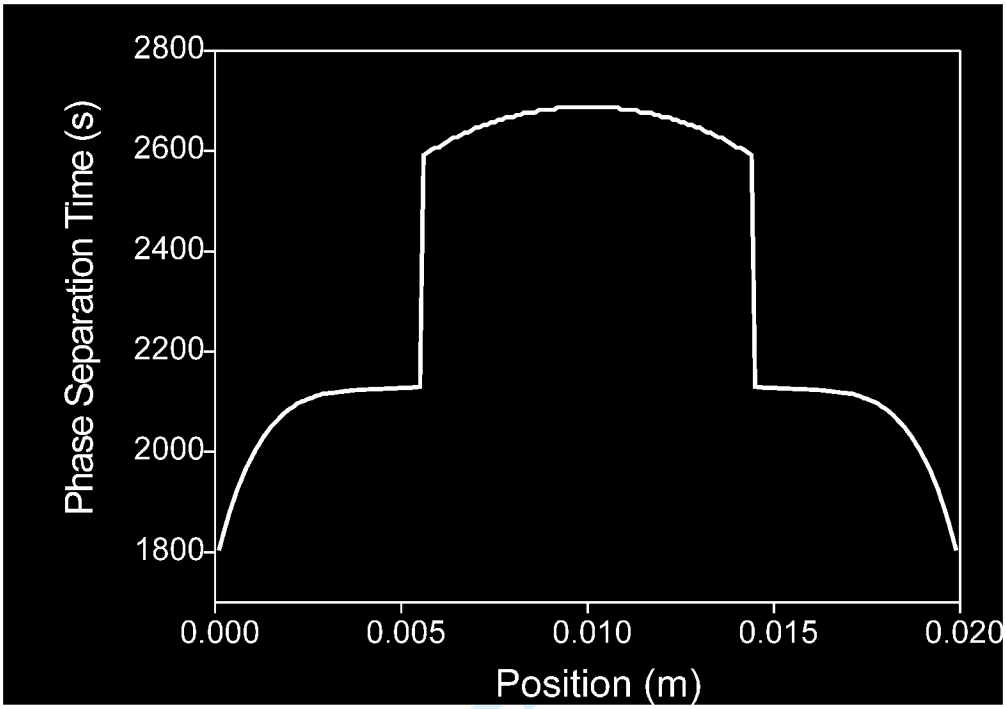
Phase Separation Time (s)
2800
2600
2400
2200
2000
1800
0.000
0.005
0.010
0.015
0.020
Position (m)